Research Article | Vol. 25, No. 16 | 7 Aug 2017 | OPTICS EXPRESS 19640

Optics EXPRESS

Optical coherence tomography and non-linear microscopy for paintings – a study of the complementary capabilities and laser degradation effects

HAIDA LIANG,[1,*] MEROPI MARI,[2] CHI SHING CHEUNG,[1] SOTIRIA KOGOU,[1] PHILLIP JOHNSON,[1] AND GEORGE FILIPPIDIS[2]

[1]*School of Science & Technology, Nottingham Trent University, Nottingham NG11 8NS, UK*
[2]*Institute of Electronic Structure and Laser, Foundation for Research and Technology Hellas, P.O. Box 1527, 71110, Heraklion, Crete, Greece*
[*]*Haida.liang@ntu.ac.uk*

Abstract: This paper examines for the first time the potential complementary imaging capabilities of Optical coherence tomography (OCT) and non-linear microscopy (NLM) for multi-modal 3D examination of paintings following the successful application of OCT to the in situ, non-invasive examination of varnish and paint stratigraphy of historic paintings and the promising initial studies of NLM of varnish samples. OCT provides image contrast through the optical scattering and absorption properties of materials, while NLM provides molecular information through multi-photon fluorescence and higher harmonics generation (second and third harmonic generation). OCT is well-established in the in situ non-invasive imaging of the stratigraphy of varnish and paint layers. While NLM examination of transparent samples such as fresh varnish and some transparent paints showed promising results, the ultimate use of NLM on paintings is limited owing to the laser degradation effects caused by the high peak intensity of the laser source necessary for the generation of non-linear phenomena. The high intensity normally employed in NLM is found to be damaging to all non-transparent painting materials from slightly scattering degraded varnish to slightly absorbing paint at the wavelength of the laser excitation source. The results of this paper are potentially applicable to a wide range of materials given the diversity of the materials encountered in paintings (e.g. minerals, plants, insects, oil, egg, synthetic and natural varnish).

OCIS codes: (110.4500) Optical coherence tomography; (180.4315) Nonlinear microscopy; (190.1900) Diagnostic applications of nonlinear optics; (140.7090) Ultrafast lasers; (110.0180) Microscopy; (140.3330) Laser damage.

References and links

1. D. Huang, E. A. Swanson, C. P. Lin, J. S. Schuman, W. G. Stinson, W. Chang, M. R. Hee, T. Flotte, K. Gregory, C. A. Puliafito, and J. G. Fujimoto, "Optical coherence tomography," Science **254**(5035), 1178–1181 (1991).
2. M. Goppert-Mayer, "Elementary processes with two-quantum transitions," Ann. Phys. Berlin **9**, 273 (1931).
3. W. Denk, J. H. Strickler, and W. W. Webb, "Two-photon laser scanning fluorescence microscopy," Science **248**(4951), 73–76 (1990).
4. W. Drexler, M. Liu, A. Kumar, T. Kamali, A. Unterhuber, and R. A. Leitgeb, "Optical coherence tomography today: speed, contrast, and multimodality," J. Biomed. Opt. **19**(7), 071412 (2014).
5. J. Kim, W. Brown, J. R. Maher, H. Levinson, and A. Wax, "Functional optical coherence tomography: principles and progress," Phys. Med. Biol. **60**(10), R211–R237 (2015).
6. M. L. Yang, C. W. Lu, I. J. Hsu, and C. C. Yang, "The use of Optical Coherence Tomography for monitoring the subsurface morphologies of archaic jades," Archaeometry **46**(2), 171–182 (2004).
7. P. Targowski, B. Rouba, M. Wojtkowski, and A. Kowalczyk, "The Application of Optical Coherence Tomography to Non-Destructive Examination of Museum Objects," Stud. Conserv. **49**, 2 (2004).
8. H. Liang, R. Cucu, G. M. Dobre, D. A. Jackson, J. Pedro, C. Pannell, C. Saunders, and A. G. Podoleanu, "Application of OCT to examination of easel paintings," Proc. SPIE **5502**, 378–381 (2004).
9. H. Liang, M. Cid, R. Cucu, G. Dobre, A. Podoleanu, J. Pedro, and D. Saunders, "En-face optical coherence tomography - a novel application of non-invasive imaging to art conservation," Opt. Express **13**(16), 6133–6144 (2005).

#301009 https://doi.org/10.1364/OE.25.019640
Journal © 2017 Received 27 Jun 2017; revised 29 Jul 2017; accepted 31 Jul 2017; published 4 Aug 2017

10. H. Liang, B. Peric, M. Hughes, A. Podoleanu, M. Spring, and S. Roehrs, "Optical coherence tomography in archaeological and conservation science - a new emerging field," Proc. SPIE **7139**, 713915 (2008).
11. P. Targowski and M. Iwanicka, "Optical Coherence Tomography: its role in the non-invasive structural examination and conservation of cultural heritage objects—a review," Appl. Phys. A **106**(2), 256–277 (2012).
12. W. R. Zipfel, R. M. Williams, and W. W. Webb, "Nonlinear magic: multiphoton microscopy in the biosciences," Nat. Biotechnol. **21**(11), 1369–1377 (2003).
13. G. Filippidis, E. J. Gualda, K. Melessanaki, and C. Fotakis, "Nonlinear imaging microscopy techniques as diagnostic tools for art conservation studies," Opt. Lett. **33**(3), 240–242 (2008).
14. G. Filippidis, M. Mari, L. Kelegkouri, A. Philippidis, A. Selimis, K. Melessanaki, M. Sygletou, and C. Fotakis, "Assessment of In-Depth Degradation of Artificially Aged Triterpenoid Paint Varnishes Using Nonlinear Microscopy Techniques," Microsc. Microanal. **21**(2), 510–517 (2015).
15. G. Filippidis, K. Melessanaki, and C. Fotakis, "Second and third harmonic generation measurements of glues used for lining textile supports of painted artworks," Anal. Bioanal. Chem. **395**(7), 2161–2166 (2009).
16. S. Psilodimitrakopoulos, E. Gavgiotaki, K. Melessanaki, V. Tsafas, and G. Filippidis, "Polarization Second Harmonic Generation Discriminates Between Fresh and Aged Starch-Based Adhesives Used in Cultural Heritage," Microsc. Microanal. **22**(5), 1072–1083 (2016).
17. G. Latour, J. P. Echard, M. Didier, and M. C. Schanne-Klein, "In situ 3D characterization of historical coatings and wood using multimodal nonlinear optical microscopy," Opt. Express **20**(22), 24623–24635 (2012).
18. G. Latour, L. Robinet, A. Dazzi, F. Portier, A. Deniset-Besseau, and M. C. Schanne-Klein, "Correlative nonlinear optical microscopy and infrared nanoscopy reveals collagen degradation in altered parchments," Sci. Rep. **6**(1), 26344 (2016).
19. G. Filippidis, G. J. Tserevelakis, A. Selimis, and C. Fotakis, "Nonlinear imaging techniques as non-destructive, high-resolution diagnostic tools for cultural heritage studies," Appl. Phys. A Mater. **118**(2), 417–423 (2015).
20. F. Faraldi, G. J. Tserevelakis, G. Filippidis, G. M. Ingo, C. Riccucci, and C. Fotakis, "Multi photon excitation fluorescence imaging microscopy for the precise characterization of corrosion layers in silver-based artifacts," Appl. Phys. A Mater. **111**, 171–181 (2013).
21. L. Broecke, Cennino Cennini, Il libro dell'arte (Archetype, 2015).
22. R. W. Boyd, *Nonlinear Optics* (Academic, 2008) 3rd Ed.
23. L. Moreaux, O. Sandre, M. Blanchard-Desce, and J. Mertz, "Membrane imaging by simultaneous second-harmonic generation and two-photon microscopy," Opt. Lett. **25**(5), 320–322 (2000).
24. J. Squier and M. Muller, "High resolution nonlinear microscopy: A review of sources and methods for achieving optimal imaging," Rev. Sci. Instrum. **72**(7), 2855–2867 (2001).
25. E. Beaurepaire, L. Moreaux, F. Amblard, and J. Mertz, "Combined scanning optical coherence and two-photon-excited fluorescence microscopy," Opt. Lett. **24**, 969–971 (1999).
26. S. Tang, T. B. Krasieva, Z. Chen, and B. J. Tromberg, "Combined multiphoton microscopy and optical coherence tomography using a 12-fs broadband source," J. Biomed. Opt. **11**(2), 020502 (2006).
27. Q. Wu, B. E. Applegate, and A. T. Yeh, "Cornea microstructure and mechanical responses measured with nonlinear optical and optical coherence microscopy using sub-10-fs pulses," Biomed. Opt. Express **2**(5), 1135–1146 (2011).
28. J. Xi, Y. Chen, Y. Zhang, K. Murari, M. J. Li, and X. Li, "Integrated multimodal endomicroscopy platform for simultaneous en face optical coherence and two-photon fluorescence imaging," Opt. Lett. **37**(3), 362–364 (2012).
29. A. Alex, J. Weingast, M. Weinigel, M. Kellner-Höfer, R. Nemecek, M. Binder, H. Pehamberger, K. König, and W. Drexler, "Three-dimensional multiphoton/optical coherence tomography for diagnostic applications in dermatology," J. Biophotonics **6**(4), 352–362 (2013).
30. C. S. Cheung, M. Spring, and H. Liang, "Ultra-high resolution Fourier domain optical coherence tomography for old master paintings," Opt. Express **23**(8), 10145–10157 (2015).
31. C. S. Cheung, J. M. Daniel, M. Tokurakawa, W. A. Clarkson, and H. Liang, "High resolution Fourier domain optical coherence tomography in the 2 μm wavelength range using a broadband supercontinuum source," Opt. Express **23**, 3 (2015).
32. H. Liang, R. Lange, B. Peric, and M. Spring, "Optimum spectral window for imaging of art with optical coherence tomography," Appl. Phys. B. **111**, 4 (2013).
33. P. M. Whitmore, X. Pan, and C. Bailie, "Predicting The Fading of Objects: Identification of Fugitive Colorants Through Direct Nondestructive Lightfastness Measurements," J. Am. Inst. Conserv. **38**(3), 395 (1999).
34. H. Liang R. Lange, A. Lucian, P. Hyndes, J.H. Townsend and S. Hackney, "Development of portable microfading spectrometers for measurement of light sensitivity of materials," International Council of Museums, Committee for Conservation (ICOM-CC) Triennial Conference Preprints, Lisbon, 1612_882 (2011).
35. A. Lerwill, A. Brookes, J.H. Townsend, S. Hackney and H. Liang, "Micro-fading spectrometry: investigating the wavelength specificity of fading," Appl. Phys. A. **118**, 457–463 (2015).
36. L. Burgio, R. J. H. Clark, and S. Firth, "Raman spectroscopy as a means for the identification of plattnerite (PbO_2), of lead pigments and of their degradation products," Analyst (Lond.) **126**(2), 222–227 (2001).
37. S. Tang, T. Krasieva, Z. Chen, G. Tempea, and B. Tromberg, "Combined multiphoton microscopy and optical coherence tomography using a 12-fs broadband source," J. Biomed. Opt. **11**(2), 020501 (2008).
38. B. C. Stuart, M. D. Feit, A. M. Rubenchik, B. W. Shore, and M. D. Perry, "Laser-Induced Damage in Dielectrics with Nanosecond to Subpicosecond Pulses," Phys. Rev. Lett. **74**(12), 2248–2251 (1995).

Optics EXPRESS

1. Introduction

As imaging and sensing technology advances with the availability of new lasers and detectors, non-invasive examination of cultural heritage is increasingly being explored for material identification, 3D surface structure and subsurface microstructure imaging. Non-invasive examination is often the only allowed scientific analysis of culturally significant historical objects. As each individual imaging modality matures, it is natural to explore multi-modal imaging approaches that exploit the complementary characteristics of each modality. In this paper, we compare two 3D optical tomographic imaging techniques, optical coherence tomography (OCT) and non-linear microscopy (NLM), and explore their complementary application on materials encountered in historic polychromic objects and in particular, historic paintings.

While Michelson's white light interferometry was invented in the 19th century, the first imaging Michelson interferometer, that is OCT, was only demonstrated in 1991 [1]. Similarly, while the concept of non-linear multi-photon fluorescence has been around since 1931 [2], the first non-linear microscope was only invented in 1990 [3]. In both cases, the first 3D tomographic applications were in biomedical imaging.

OCT is based on the Michelson interferometer where the sample arm probing depth is obtained through white light interferometry by combining the signals reflected from the sample and reference arms. The intensity of an OCT image reflects the optical scattering and absorption properties of the material. Since scattering and reflection is a result of refractive index changes, OCT is particularly sensitive to refractive index inhomogeneity in a material. Currently, the majority of OCT applications are in biomedical imaging of the eye and other biological tissues such as the skin [4,5]. Since 2004, OCT has been successfully applied to a variety of cultural heritage [6–9] from traditional portable paintings, illuminated manuscripts on parchments, wall paintings, vitreous materials, leathers, papers to jade and carved rock art panels [10,11].

Non-linear image contrast modalities are well-established techniques for biological research [12], however at the same time, they have been shown to be powerful diagnostic tools for cultural heritage studies. Specifically, recent studies have demonstrated the potential of these techniques for depth resolved imaging of materials in cultural heritage such as varnishes [13,14], lining glues [15,16], historical coatings [17], parchments [18], paint [19] and corrosion layer in metal-based artefacts [20]. The non-linear microscopy modalities employed were multi-photon excitation fluorescence, second and third harmonic generation.

Multi-photon excitation fluorescence is a non-linear optical procedure where the nonlinear process depends on the intensity of the incident laser irradiation. Multi-photon excitation fluorescence measurements are able to give some indication of the chemical composition of artefacts. The simplest case is two-photon excitation fluorescence. During two-photon excitation fluorescence, one photon having energy approximately equal to half the energy difference between the excited and the ground state of a fluorescent molecule interacts with the electron in order to excite it to an intermediate virtual state where it will remain for an extremely short time (1 femtosecond). If the spatial and temporal density of the incident beam is high enough, there is a finite probability that a second photon will interact with the electron of the virtual state resulting in the transition of the electron to the excited state. The consequent de-excitation of the electron returning to the ground state emits a single fluorescent photon of higher energy to the incident photons.

In western European paintings, varnish layers are commonly applied to a painting to improve aesthetic properties as well as for the protection of the paint layer [21]. Most of the varnish layers are highly transparent in the visible and near infrared (NIR) region of the spectrum, while the paint layers can absorb at the excitation laser wavelength (usually in the NIR ~1064 nm). Therefore, in contrast to the varnishes where multi-photon absorption is the predominant mechanism for fluorescence emission, the fluorescence from painting materials can be the result of a combination of single and multi-photon absorption processes. These

Optics EXPRESS

different absorption properties of the above components have also an impact on the nature of their respective damage mechanisms. It is relatively more probable to cause unwanted photo-damage effects when paint layers are examined.

Optical second or third harmonics generation are coherent scattering phenomena that have a non-linear dependence on the incident light beam intensity. If N number of photons (2 for the case of second harmonic generation and 3 for third harmonic generation) of energy $h\omega$ interact within the focal volume of a material, they can be combined effectively to emit a photon of energy $Nh\omega$. The N-th harmonic generation intensity scales with the intensity of the fundamental incident radiation I as I^N. During these non-linear scattering phenomena, no energy is deposited in the medium and the new photons are generated through a single step quantum process [22]. Thus, the interacting material acts as an energy converter of the incident photons. Second harmonic generation is produced only in non-centrosymmetric molecules (starch granules, collagen) and hence providing material information and a unique image contrast [23]. On the other hand, third harmonic generation occurs in any medium and is therefore more versatile. However, third harmonic generation is sensitive to local inhomogeneities such as in the third order non-linear susceptibility $\chi^{(3)}$, refractive index and dispersion. Third harmonic generation signal arises when the laser beam is focused at the interface of two optically different materials [24]. This property allows the third harmonic generation to distinguish and image structural inhomogeneities within the confocal parameter limitation, avoiding the use of fluorescent dyes. Consequently, third harmonic generation constitutes a high resolution diagnostic tool for structural and morphological information of different samples.

Non-linear imaging microscopy shows many advantages compared to other microscopy methods. It is capable of intrinsic three dimensional (3D) subsurface sectioning while still avoiding damage to objects through photobleaching or phototoxicity phenomena in the out-of-focus area. NLM harmonic generation in the second and third harmonic generation ensure minimal sample disturbance, as they are scattering phenomena with little energy being deposited in the sample. However, the same high intensity beam that enables second and third harmonic generation, may also be absorbed through other non-linear processes such as multi-photon excitation fluorescence which can cause laser induced damage.

A significant advantage of NLM is that, all the aforementioned signals are generated simultaneously in the focal volume of the examined object. Thus, they provide unique complementary information related to the chemical composition of the sample such as the centrosymmetry of its molecules (through second harmonic generation measurements) and the structural delineation of the material. In general, non-linear imaging modalities present limited depth information, but better transverse resolution and similar axial resolution when compared to OCT. OCT can give the same high lateral resolution as NLM when using the same objective lens. This kind of OCT is sometimes called optical coherence microscopy.

Beaurepaire et al. [25] were the first to achieve complementary measurements of NLM and OCT for biomedical imaging, noting that OCT gives the structural information from the backscattered photons while NLM gives the functional information through the non-linear fluorescence generation. Tang et al. [26] demonstrated the combined application of two-photon excitation fluorescence, second harmonic generation and OCT in one system for tissue imaging using a 12-fs laser. The combination of NLM and OCT in one system is natural, since the fs laser provides both the necessary high peak intensity for the generation of non-linear effects such as two-photon excitation fluorescence and second harmonic generation, and the necessary broad bandwidth for the high axial resolution requirements of an OCT. They demonstrated that two-photon excitation fluorescence was from cellular structure, while second harmonic generation signal came from extracellular matrix structure. In comparison, OCT signals were collected from the back-scattered photons from variations in refractive indices, and thus gave the full structure of both the cell and the extracellular matrix. In addition, OCT images showed more collagen than the second harmonic generation image. It was also noted that there is an optimum pulse width for OCT and NLM operation, since the broad source bandwidth (i.e. shorter pulse) to improve OCT axial resolution may reduce the efficiency of two photon absorption, especially if the bandwidth is larger than the fluorescence emission bandwidth. Wu et al. [27] also demonstrated an integrated NLM/OCT system for the study of mechanical properties of cornea; Xi et al. [28] developed an integrated endoscopic system combining NLM/OCT. More recently, Alex et al. [29] have combined 3D scanning of OCT and two-photon excitation fluorescence for dermatology and demonstrated the advantages of exploiting the complementary contrast of the two techniques. In this paper, we will examine for the first time the complementary imaging capabilities offered by OCT and NLM for non-biological materials such as a diverse range of painting materials.

While the effects of laser induced degradation due to both NLM and OCT have been examined in biomedical applications extensively, they have not been examined systematically in cultural heritage applications. Some of these studies have used visual examination with optical microscope to examine obvious damages or simply quoting the results in biomedical applications. However, many changes in materials are not readily discernible using an optical microscope and the susceptibility to laser damage in biomedical material may be totally different from those of cultural heritage. In this paper, we will examine systematically the potential effects of laser degradation in these two imaging modalities.

2. Imaging systems

2.1 Optical coherence tomography systems

An in-house developed ultra-high resolution spectrometer-based Fourier domain OCT at a central wavelength of 810 nm with an axial resolution of 1.2 microns (in varnish or paint) and transverse resolution of 7 microns was used to image the more transparent samples [30], while an in-house developed longer wavelength spectrometer-based Fourier domain OCT at a central wavelength of 1960 nm with an axial resolution of 6 microns (in varnish or paint) and transverse resolution of 17 microns was used to image the more opaque (i.e. high scattering or absorption coefficient) samples [31]. The 810 nm OCT used a NKT SuperK versa supercontinuum source [30] and the 1960nm OCT used a custom built supercontinuum source [31]. Details of the OCT systems were described in previous papers [30, 31]. In both cases, the power incident on the sample was ~1 mW. It took 10 ms for a cross-section scan (500 depth profiles or A-scans) using the OCT at 810nm, while it takes 200 ms for the same scan using the long wavelength OCT at 1960 nm. The integration times per depth profile were 10μs and 100μs for the 810 nm and 1960 nm OCTs respectively. The OCT images presented in this paper were taken without any averaging unless otherwise specified.

2.2 Non-linear microscopy set-up

Tightly focused femtosecond laser pulses represent ideal sources for non-linear microscopy applications. A single 200 fs laser beam at 1028 nm (Amplitude systems) was used for the performance of the non-linear measurements (multi-photon excitation fluorescence, second harmonic generation, third harmonic generation). The in-house developed apparatus employed has been described in previous papers [14,16,19]. An average power of 25 mW at the sample plane was used (energy per pulse 0.5nJ). Multi-photon excitation fluorescence signals were collected in the backward direction using a photomultiplier tube (PMT Hamamatsu R4220).

Third harmonic generation signals can be detected simultaneously with the multi-photon excitation fluorescence signal emitted in the forward direction, by employing a colored glass filter (U 340nm Hoya) and a second PMT. Typical time duration for a single spot non-linear measurement is of the order of a few seconds; while a cross-sectional scanning takes just under 2 min. A 20x, 0.80 numerical aperture (NA) objective lens (Carl Zeis, Plan

Optics EXPRESS

Apochromat) was employed for the tight focusing of the laser beam onto the sample. The transverse and axial resolutions of our setup are ~770 nm and 2μm, respectively.

3. Materials

A range of historic artist's paints prepared on a variety of substrates were examined by both OCT and NLM. These include inorganic pigments, i.e. minerals, organic pigments derived from plants and insects, binding medium such as oil and egg as well as natural and synthetic varnish. The pigments were selected to have low absorption at the laser excitation wavelength of 1028 nm for the NLM to minimize potential laser degradation effects. Table 1 shows the list of 28 pigments thus selected that were mixed with linseed oil or egg tempera. These were painted in 2006 by the National Gallery in London on both glass microscope slides and boards sized with chalk in rabbit skin glue [32]. Samples of pure binding media including linseed oil, egg tempera, animal glue and gum Arabic were also applied on glass. Samples of varnish applied on glass including fresh mastic, dammar, regalrez, paraloid B72 and a couple of artificially and naturally aged mastic varnish samples that has yellowed and gone hazy were also tested.

Table 1. Pigment samples

Pigment	Binder	Pigment	Binder
Art. Ultramarine	Oil	Indigo	Oil & egg
Smalt (light)	Oil & egg	Chrome Red	Oil & egg
Vermilion 3	Oil & egg	Sappanwood Lake	Oil
Lapis Lazuli	Oil	Italian Golden Ochre	Oil
Red Ochre	Oil	Cochineal Lake	Oil & egg
Red Lead	Oil & egg	Lac Lake	Oil
Lead White	Oil	Cadmium Red	Oil
Lemon Yellow	Oil & egg	Cobalt Yellow	Oil
Lead Tin Yellow	Oil	Dyer's broom Lake*	Oil
Chrome Yellow	Oil & egg	Naples Yellow (light)*	Oil
Cadmium Yellow (light)	Oil	Viridian Green	Oil & egg
Azurite grade1	Oil	Zinc White*	Oil
Cobalt blue	Oil	Weld Lake	Oil
Titanium White	Oil	Rose Madder	Oil & egg

*indicate no fluorescence detected with the NLM

4. Complementary imaging using OCT and NML

OCT measures optical thickness and to convert to real thickness, we need to divide by the refractive index. In contrast, for the NLM, the real thickness is roughly equal to the measured thickness multiplied by the refractive index. Refractive indices of the materials can be accurately measured with OCT using those samples on flat glass substrates. As expected, the refractive indices for the varnish samples were all measured to be ~1.5 at 810nm. Figure 1 shows an example of OCT and NLM imaging of a multi-layer varnish sample. The layers of mastic and vinavil varnish are distinguished by their optical scattering properties in the OCT image. Vinavil is moderately scattering, while mastic is transparent in the OCT image. In the two-photon excitation fluorescence image as in the OCT image, the vinavil layer is ~2 times as thick as the mastic varnish layer. The combined thickness of the two layers of varnish vary between 78 and 95 microns over the OCT field of view of 5mm which is consistent with the third harmonic generation measured thickness of 90-95 microns over a field of view of 150 microns. The vinavil layer fluoresces less than the mastic layer in the two-photon excitation fluorescence image. While it is impossible to distinguish the fresh mastic layer from the glass layer in the OCT image apart from the interface between the two layers, the NML shows clear difference since mastic shows strong fluorescence but glass does not. Similar to OCT, third harmonic generation is sensitive to refractive index discontinuities and hence the interfaces between the different media are clearly delineated. Third harmonic generation signals from the interfaces between the different media offers more precise measurements of the thickness of mastic, vinavil and glass layers than two-photon excitation fluorescence. It should be noted that vinavil is not a common varnish for paintings, but in this case it was convenient to use this example to contrast the different imaging modalities.

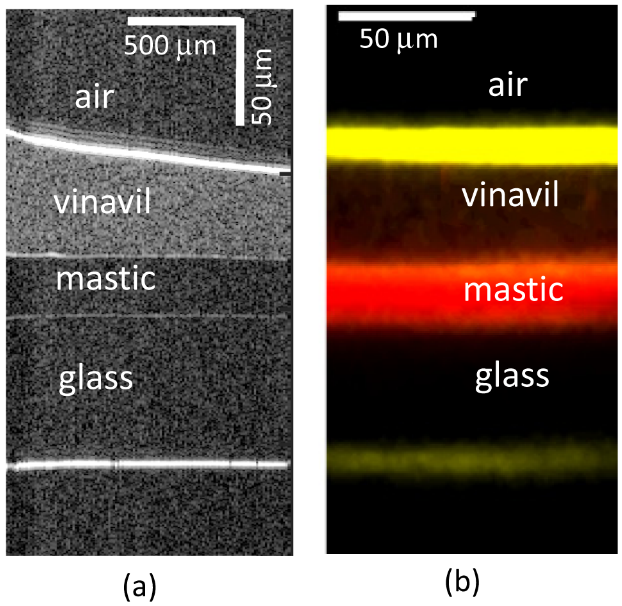

Fig. 1. a) OCT image of two layers of different varnish (vinavil on mastic) painted on a thin glass slide. b) NLM multi-modal image of the same sample where the multi-photon excitation fluorescence (red) and third harmonic generation (yellow) images are superposed. Note that the OCT image aspect ratio is not 1:1, but the NLM images are 1:1 in aspect ratio.

Most fresh natural varnishes, such as dammar and mastic, are completely transparent in OCT images and therefore impossible to tell the difference. However, their multi-photon excitation fluorescence intensities are rather different as shown in Fig. 2, with mastic more strongly fluorescent than dammar, even though both dammar and mastic give 3 photon fluorescence [14]. While this information is useful on fresh varnish samples, the behavior of aged varnish samples is much more complex. The intensity of single photon fluorescence is known to increase with the ageing of the varnish, while it has been observed from multi-photon excitation fluorescence imaging that the intensity of fluorescence increases with depth as varnish ages [14].

Optics EXPRESS

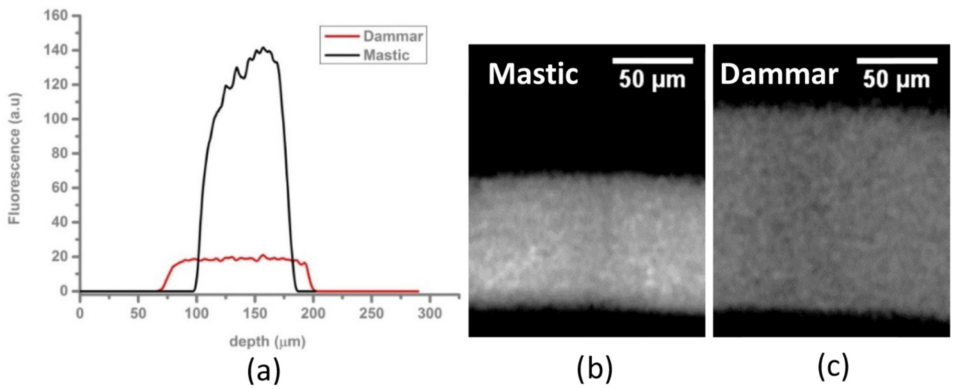

Fig. 2. a) Fluorescence intensity versus depth for samples of dammar and mastic varnish on glass; the thicknesses of dammar (red curve) and mastic (black curve) are measured from multi-photon excitation fluorescence images of b) fresh mastic and c) fresh dammar. The images have 1:1 aspect ratios.

When the paint samples on glass (Table 1) were imaged with NLM and OCT, it was found that in general OCT was able to penetrate deeper into the sample. Figure 3 shows the multi-photon excitation fluorescence image of sappanwood lake in oil painted on a glass slide compared with the OCT image of the same sample. The 810 nm OCT image shows the full thickness of the layer to be 100-200 microns with clear interface between the paint layer and the glass substrate, while the multi-photon excitation fluorescence only revealed the top 70 micron of the layer with gradually diminishing signal with increased depth. Figure 4 shows that the full depth of the lapis lazuli layer to be ~100-150 microns as measured with the 1960nm OCT, while the multi-photon excitation fluorescence image only shows the top 30 micron. Most pigments become more transparent in the near infrared at longer wavelength [32], therefore the longer the central wavelength the better depth of penetration for OCT imaging, which was why the full thickness of the lapis lazuli sample was revealed in the 1960nm OCT but not in the 810nm OCT image (Fig. 4(c)). In the case of multi-photon excitation fluorescence imaging, even if the excitation wavelength is in the near infrared at a long wavelength and therefore likely to penetrate deeper into the sample to excite fluorescence, the multi-photon fluorescence emission would still be at a much shorter wavelength in the visible range and therefore likely to be absorbed or scattered by the material above where it originated and not be detected. This may explain why the multi-photon excitation fluorescence image of the sappanwood lake sample (a red lake pigment which absorbs light at wavelength <650nm) did not show the full depth even though it is transparent at the laser excitation wavelength of 1028nm.

In some cases, NLM showed signs of laser induced degradation. It was particularly obvious in the case of vermilion and red lead where a black spot was found after the scanning. In the following section, we will examine the effect of the laser beam on these common pigments that are selected for their low absorption at the laser excitation wavelength of 1028 nm.

Optics EXPRESS

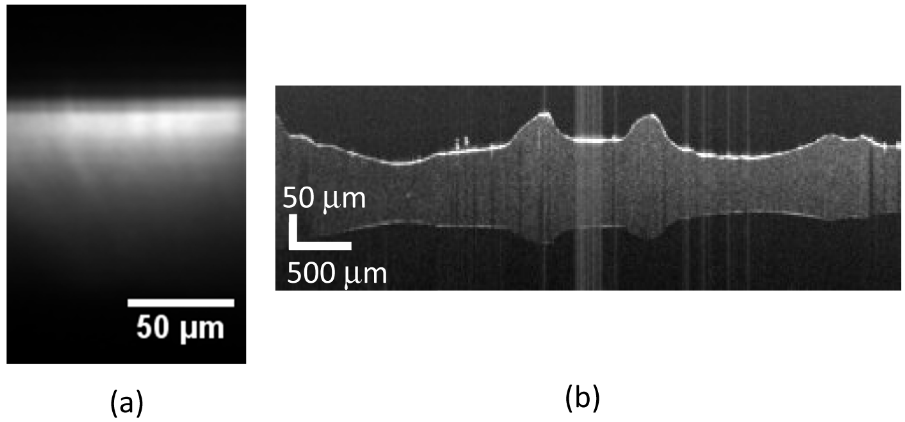

Fig. 3. Sappanwood lake in oil painted on glass: a) multi-photon excitation fluorescence image (1:1 aspect ratio) showing the top ~70 microns of the paint layer and b) 810nm OCT image (average of 10 frames) showing the paint layer thickness of 100-200 microns.

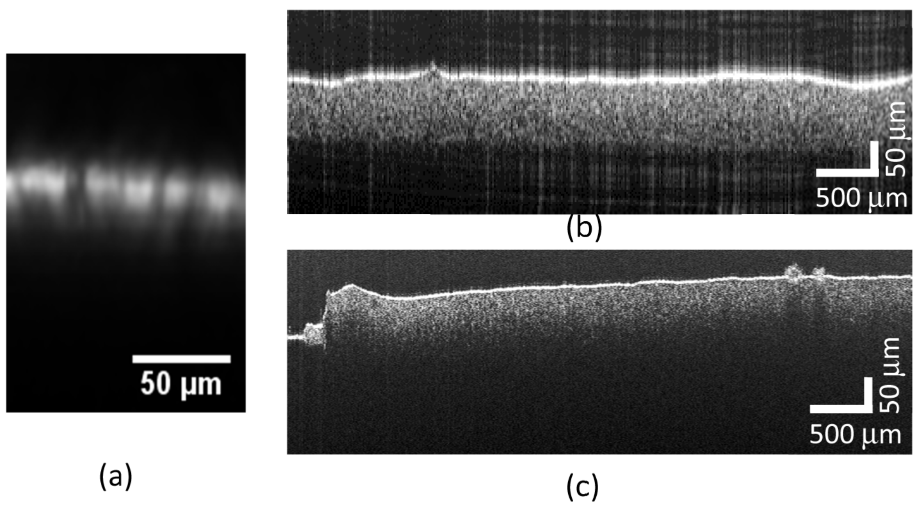

Fig. 4. Lapis Lazuli in oil painted on glass: a) multi-photon excitation fluorescence image (1:1 aspect ratio) showing a thickness of ~30 microns; b) 1960 nm long wavelength OCT image showing a thickness of ~100-150 microns and c) 810 nm UHR OCT image showing the paint layer on glass (left most side shows the bare glass surface but the paint/glass interface is not seen due to absorption).

5. Laser induced degradation

While laser induced degradation effects were examined for OCT and NLM in detail in biomedical applications, no systematic experiments have been conducted for cultural heritage materials yet. The precautions taken and safe use of these techniques were guided by experience in biomedical applications. In the case of OCT, estimates of the intensity and fluence were also used to justify the safety of the method and indeed to date there has not been any known laser damage produced as a result of OCT imaging on samples or on any real objects. In NLM, visual observation is often used to confirm that no damage is done. However, degradation is sometimes more subtle than what is visually perceptible under a microscope. Table 2 compares the intensity and fluence of typical laser sources used in OCT, NLM, micro-Raman as well as the Xenon light source used in the well-known (in preventative conservation) in situ accelerated light ageing technique microfade [33–35]. Detailed studies of laser induced damage for micro-Raman spectroscopy has been conducted (e.g. Burgio et al. [36]) and the tabulated values for micro-Raman are the maximum intensity normally used to avoid laser induced damage. Both Raman and OCT normally use continuous wave laser sources (or near continuous wave in the case of supercontinuum lasers) and it is clear that while OCT intensity is only slightly lower than micro-Raman, the fluence is at least 5 orders of magnitude lower due to the rapid scanning process and the high sensitivity of the technique. Compared with the broadband white light source used in microfade, the intensity of the laser source in OCT is 3 orders of magnitude higher but the fluence is at least 4 orders of magnitude lower. In comparison, NLM is 3 to 7 orders of magnitude higher in intensity depending on whether we take the peak or average pulse intensity and 3 orders of magnitude less in fluence compared with micro-Raman. Both intensity and fluence affect the light induced damage, but wavelength is another important factor. For the laser-based techniques, we can compare the effects at similar wavelength, but the light source in microfade is usually broadband covering the entire visible range. Narrow band wavelength dependent fading behavior of pigments have also been studied using microfade providing comparison with a non-laser based source (e.g [35]). Both OCT and NLM tend to operate in the near infrared, unlike microfade and some Raman microscopes.

Table 2. Light intensity and fluence comparison

	P_{av} (mW)	P_{max} (W)	Spot size (µm)	dwell time (s)	I_{av} (W/cm^2)	I_{max} (W/cm^2)	fluence (J/cm^2)
Microfade	2		500	600	1		600
OCT	1		10	10^{-5}	1.3×10^3		0.013
Raman	1		5	1	5.1×10^3		5100
NLM*	25	2500	1.5	4×10^{-6}	1.3×10^6	1.3×10^{11}	5.2
ns-pulsed laser**		2×10^4 to 1×10^7	3000	5×10^{-9}		2.8×10^5 - 1.4×10^8	0.0014 to 0.7

*The fluence per pulse for NLM is 0.026 J/cm2. In each spot we have 200 pulses so the total fluence is calculated at 5.2 J/cm2 for our NLM measurements.

**Continuum Nd:Yag laser 1064nm, 5ns pulse width, delivering one pulse at a time with maximum 50 mJ/pulse and minimum 0.1 mJ/pulse; here we give the corresponding range of fluence for 1 pulse; 8 pulses gives the same fluence as one of our NLM scan (i.e. 200 pulses per spot)

5.1. Nonlinear microscopy

Ideally laser induced damage due to NLM should have been measured with the NLM setup using the same laser, however, the space constraint at the objective and the detection side of the NLM made it difficult to have a stable setup. As an alternative, the setup in Fig. 5 was used where a collimated 3 mm diameter beam of Nd:Yag ns-pulsed laser at 1064 nm was used to irradiate a sample at normal incidence pulse by pulse while a probe with a spot size 0.45×0.75 mm^2 on the sample is aligned at ~45° angle to the laser beam to collect the reflectance spectrum within the laser irradiated spot of the sample after each pulse. The probe collects the reflectance spectrum in a retro-reflection configuration using a low power Tungsten light. The parameters of this laser is given in Table 2 and it can be seen that 8 pulses of this laser at maximum energy per pulse give the same fluence as 200 pulse of the fs laser used in the NLM to illuminate one spot in a NLM scan. The peak intensity of this ns-pulsed laser is 3 orders of magnitude lower than the NLM laser. The slight difference in wavelength

Optics EXPRESS

between this laser (1064nm) and the NLM laser (1028nm) should not influence the results as none of the samples tested had narrow absorption features near 1028 nm or 1064 nm. After each irradiation of the laser pulse, a reflectance spectrum is collected by the Ocean Optics HR2000 spectrometer with a low intensity Tungsten light as the illumination source. Figure 6(a) shows the stability of the spectrometer, probe and Tungsten light system over a period longer than the test period of laser damage experiments per sample.

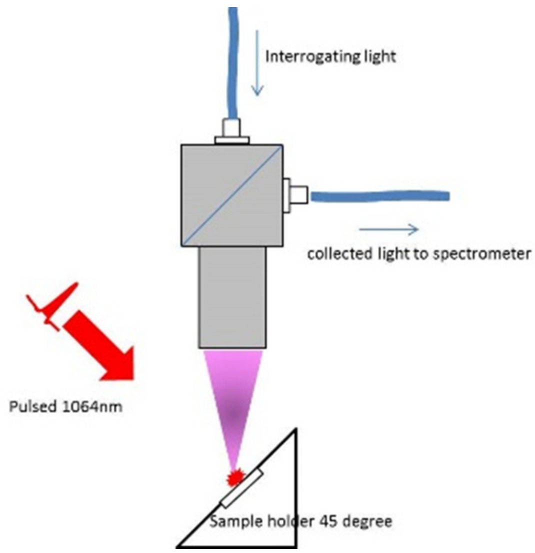

Fig. 5. Experimental setup for measuring laser induced degradation in the paint and varnish samples.

Amongst the glass substrate samples, the relatively transparent materials such as fresh binding media, fresh varnish and some of the lake pigments in oil binder did not change after exposure to 8 pulses (e.g. Fig. 6(b)). However, all samples that are significantly scattering, from the highly scattering samples, such as titanium white and zinc white, to the less scattering aged varnish which had a hazy appearance, showed significant changes in their reflectance spectra after the laser irradiation at full power (e.g. Fig. 6(c)). All samples that are significantly absorbing also showed signs of degradation. It is interesting that a transparent lake pigment in oil painted on a board prepared by a white chalk in rabbit skin glue ground layer also showed significant change after the laser irradiation. This is presumably because the paint layer is transparent and therefore the laser beam did not lose much energy inside the paint before it reached the highly scattering white chalk layer beneath and thus degrading the chalk layer. This would suggest that special care must be taken when we use NLM on any real paintings and polychromic objects, since the paint layers that are highly scattering or absorbing are susceptible to laser damage and those that are transparent exposes the lower layers to laser damaged.

Optics EXPRESS

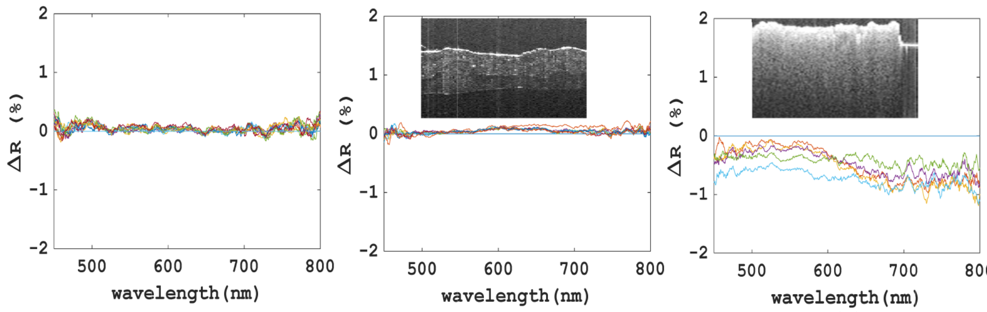

(a) (b) (c)

Fig. 6. Difference spectra for reflectance of a) a white standard without laser irradiation over a period of 10 mins showing the stability of the spectrometer system; b) a cochineal oil paint on a glass slide after each Nd:Yag laser pulse at full power; c) a cochineal egg tempera paint on a glass slide after each laser pulse at full power. The insets are 810nm OCT images of the samples showing the cochineal oil paint is fairly transparent but the cochineal in egg tempera paint is much more scattering.

After performing NLM on the red lead oil paint sample, burnt out black spots were observed in the sample, therefore we also examined the damage threshold intensity on a red lead oil paint using the setup in Fig. 5. Damage was detected by the changes to the reflected spectrum after the exposure to just one pulse of the ns-pulsed laser at 2% of the full pulse energy, but when the pulse energy was reduced to 0.6% of the maximum energy, that is an intensity of 0.8×10^{6} W cm^{-2}, no damage was detected even after 100 pulses (Fig. 7) suggesting that the damage fluence is much lower for higher intensity irradiation. This damage threshold in intensity at 1064 nm is consistent with the red lead threshold for Raman at the same wavelength using a continuous wave laser [36].

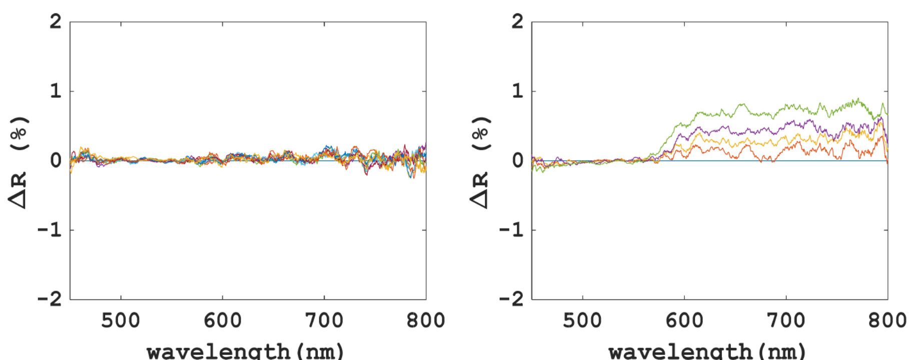

(a) (b)

Fig. 7. Reflectance spectra of a layer of red lead oil paint on a glass slide after irradiation with the Nd:Yag ns pulsed laser: a) after 1 to 100 pulses at 0.3 mJ per pulse (or 0.6% of full power), b) after 1 to 4 pulses at 1 mJ per pulse (or 2% of full power).

Finally, it was interesting to examine if there was any laser induced damage using the ns pulsed laser on fresh parchment since there has been reports of NLM examination of historic parchment [18]. It was found that, at least for fresh new parchments, no laser induced damage was detected after 8 pulses at full power. This is perhaps not surprising as parchment is made of skin and we know from biomedical applications that NLM does not cause damage to skin tissues. Significant reduction in laser induced damage can be expected i) if more sensitive detectors are used to reduce the integration time and faster scanners (e.g. lower inertia galvanometric mirrors) are used to reduce the scanning time; and ii) having shorter pulse incident at the sample plane achieved by using a shorter fs pulsed laser and implementing appropriate pulse dispersion compensation. Shorter pulse means higher peak intensity for the same pulse energy and therefore higher efficiency at generating NLM signal $(\propto t^{-1})$ [37]. For transparent solids, it is known that the damage fluence threshold also decreases with shorter pulses and higher peak intensity as t^{m}, where $m \sim 0.5$ for ns and ps pulses, however, for shorter pulses $m < 0.5$ [38]. Therefore, it is likely that the NLM signal generation increases much faster with decreasing pulse duration than the likelihood of damage due to higher intensity pulses, especially for shorter fs pulses. This means that by employing shorter fs pulses, we may be able to reduce the fluence to keep it below the damage threshold while still gather enough NLM signals at the same signal to noise ratio. It is important to note that laser damage due to the shorter fs laser pulses are fundamentally different from the ns pulsed lasers. The ns laser damage tends to affect a larger area through heat damage such as melting, while the shorter fs laser damage tend to be restricted to the very center of the beam dominated by collisional and multi-photon ionization [38]. Short pulse fs laser induced damage is often harder to detect due to the small size of the damage, and therefore it is best to incorporate laser damage monitoring within the NLM to allow the reflectance spectra from the irradiated spot to be measured through the same objective or exam the scanned area afterwards with a scanning electron microscope (SEM).

5.2 Optical coherence tomography

Some of the most light sensitive pigments such as realgar and Prussian blue were examined [34,35]. The samples were repeatedly scanned with the 810nm OCT (the spectral range of the supercontinuum source incident on the sample is 600-1000 nm) for 400 times in an area equal to the spot size of our fibre-optic spectrometer probe (3 mm diameter). The mismatch between the OCT spot size (7 microns) and the spot size of the spectrometer meant that it was necessary to scan the OCT over the area of the spectrometer probing spot size. No change was detected by the spectrometer even after 400 times the normal exposure for OCT imaging.

6. Conclusions

OCT is a relatively mature technique for the non-invasive 3D imaging of subsurface microstructure of materials in cultural heritage compared with NLM. The axial resolution of OCT and NLM are similar, while OCT in general is used with lower transverse resolution and larger transverse field of view. The transverse resolution of NLM by nature needs to be high in order to have high axial resolution and high intensity for the generation of non-linear phenomena. OCT is typically 3 to 4 orders of magnitude faster in image acquisition and has larger penetration depth than NLM. In this paper, the applicability of NLM to the non-invasive imaging of polychromic objects, such as historic paintings, was examined and compared with OCT imaging. Both OCT and third harmonic generation are sensitive to refractive index discontinuity at layer interfaces. Multi-photon excitation fluorescence by nature offers image contrast between layers with different non-linear fluorescence properties, while OCT image contrast is given by the difference in optical scattering and absorption properties between the layers. As an example, it was demonstrated that while OCT cannot distinguish between two types of equally transparent varnish, multi-photon excitation fluorescence signal showed an intensity variation between these varnishes.

This paper also examines in detail, for the first time, the potential laser induced damage for OCT and NLM. It was found that the usual laser intensity employed in OCT imaging does not cause any damage even after the same spot is illuminated for 400 times longer than necessary to collect the image. In contrast, NLM was found to cause laser-induced damage even for samples selected specifically for their low absorption at the laser excitation wavelength. A ns-pulsed Nd:Yag laser with maximum intensity three orders of magnitude less than the NLM fs-laser was used to irradiate the paint and varnish samples a pulse at a time, until the fluence was equal to the exposure per spot of the NLM scans (200 pulses). It was found that except for those samples that are transparent such as fresh varnish and some lake glazes, laser-induced degradation was detected. All samples that showed optical scattering, even aged hazy varnish (i.e. increased optical scattering), were found to degrade under the laser irradiation. It was found that change was detected when a transparent layer is painted above a white ground (i.e. strong scattering layer) or carbon black underdrawing (i.e. high absorption). This shows that in practice the use of NLM on real painted objects is limited due to likely laser induced degradation caused by the high intensity of the laser required to generate non-linear phenomena. It is hoped that the unwanted degradation effects might be reduced by employing shorter pulse duration lasers and more sensitive detectors and faster scanning mechanisms. In the future, we can modify the NLM to use a 20 fs pulsed laser with appropriate dispersion compensation and incorporate a monitoring reflectance spectroscopy system that shares the same objective as the NLM for laser damage monitoring to find the optimum parameters for NLM imaging of painted objects.

Funding

EU Horizon 2020 program LASERLAB-EUROPE (H2020-INFRAIA-654148); EU Horizon 2020 program IPERION-CH (H2020-INFRAIA- 654028); UK Arts and Humanities Research Council (AHRC) and Engineering & Physical Sciences Research Council (EPSRC) Science & Heritage Program (Interdisciplinary Research Grant AH/H032665/1).

Acknowledgments

The authors acknowledge K. Melessanaki of FORTH for her expert assistance in the preparation of varnish samples and the National Gallery in London for the painted samples. Funding has been provided by EU Horizon 2020 programs LASERLAB-EUROPE (H2020-INFRAIA-654148), IPERION-CH (H2020-INFRAIA- 654028) and UK AHRC and EPSRC Science & Heritage Program (Interdisciplinary Research Grant AH/H032665/1). Phillip Johnson is grateful for a Nottingham Trent University Physics Undergraduate Research Scholarship. Sotiria Kogou is grateful for a Nottingham Trent University PhD scholarship.